

## Si(111)- $7\times 7$ surface: Energy-minimization calculation for the dimer—adatom—stacking-fault model

Guo-Xin Qian and D. J. Chadi

Xerox Palo Alto Research Center, Palo Alto, California 94304

(Received 9 July 1986)

An energy-minimization calculation was performed on the Si(111)- $7\times 7$  surface reconstruction model proposed by Takayanagi *et al.* The structure contains dimers, adatoms, and stacking faults (DAS) in the surface layer. The DAS model has 19 dangling bonds and 12 “top-site” adatoms per  $7\times 7$  unit cell. Hellmann-Feynman forces were used to relax adatom and three layers of a five-layer slab consisting of 249 atoms. The surface energy is found to be 0.40 eV per  $1\times 1$  cell lower than that of an ideal and unrelaxed Si(111) surface, as compared to 0.36 eV for the  $\pi$ -bonded chain structure for the  $2\times 1$  cleaved surface. This is the lowest surface energy calculated for the Si(111) surface. Atomic configurations were obtained for the completely relaxed system. The calculated surface electronic density of states and the atomic origin of the surface electronic structure are in good agreement with experimental data. The results of similar calculations for Si(111)- $5\times 5$  DAS and Si(111)- $c(2\times 8)$  dimer-chain models are compared and discussed.

### I. INTRODUCTION

The reconstruction of the Si(111)- $7\times 7$  surface has been a subject of continued interest for more than a quarter of a century. Schlier and Farnsworth first observed its reconstruction through low-energy electron diffraction (LEED) in 1959,<sup>1</sup> and a large number of models have been proposed since then. A few examples are the vacancy model,<sup>2</sup> adatom models,<sup>3,4</sup> the rippled-surface model,<sup>5,6</sup> “milk-stool” model,<sup>7</sup> the buckled model,<sup>8</sup> and the pyramidal-cluster model.<sup>9,10</sup> Adatom models became very appealing after Binnig *et al.*<sup>4</sup> first observed 12 adatomlike features per unit cell through the novel technique of scanning tunneling microscopy (STM). Before STM, McRae *et al.*<sup>11</sup> had suggested that half of the  $7\times 7$  unit cell underwent a stacking-sequence fault, resulting in dimerization of atoms along the edges of the triangular unit cell. On the basis of ion-channeling experiments Bennett *et al.*<sup>12</sup> provided strong evidence for the stacking-fault sequence. More recently Takayanagi *et al.*<sup>13,14</sup> proposed a reconstruction model based on analyses of transmission electron diffraction (TED) and microscopy (TEM) data. Their model incorporates all the above-mentioned features: dimerization of the second-layer atoms, 12 adatoms per  $7\times 7$  unit cell, stacking faults, and stacking-sequence faults (DAS). The new DAS model is very attractive because it contains only 19 dangling bonds per unit cell. There are, however, very large angular distortions. A model total-energy calculation<sup>15</sup> for the DAS model shows it to be energetically favorable. In this paper, we report on the results of energy-minimization calculations based on the semiempirical tight-binding method.

The organization of the paper is as follows: Section II is devoted to the description of the DAS model. In Sec. III, the semiempirical tight-binding method is reviewed and extended to systems with adatoms involving large angular distortions. The results of our tight-binding calculations

for the Si(111)- $7\times 7$  and  $5\times 5$  DAS models are discussed in Sec. IV. In Sec. V we report on the results of our total-energy calculations for a Si(111)- $c(2\times 8)$  dimer-chain model. A brief summary is presented in Sec. VI.

### II. DAS MODEL FOR THE Si(111)- $7\times 7$ SURFACE

The DAS model for the Si(111)- $7\times 7$  surface is discussed in Refs. 13 and 14. Figure 1 is a top view of this model which illustrates its basic features. The unit-cell boundaries are marked by dotted lines. In each cell, the 12 adatoms are represented by dotted circles, and the 42 surface-layer atoms are represented by large open circles. The adatoms lie above second-layer atoms (represented by small-size circles when not hidden by adatoms). As can be seen the adatoms are not on “hollow” sites but on “top” sites directly above second-layer atoms. Thirty-six of the 42 surface-layer atoms are bonded to adatoms and their broken bonds are saturated. The remaining six surface-layer atoms which are not bonded to adatoms maintain their threefold coordination. The second-layer atoms dimerize along the boundaries of each triangular subunit. Nine dimers are present in each unit cell. At the corner of each cell a bonded ring of 12 atoms surrounding a large “hole,” consistent with STM images of the surface,<sup>4</sup> can be seen. Atoms below the second layer are relaxed from their normal positions but do not show reconstructions. The unblocked third-layer atoms are represented by large dark circles; most third-layer atoms are directly beneath second-layer atoms and are hidden from view. The atoms in the adatom layer and in the first two surface layers are approximately symmetric with respect to the short diagonal, thus the stacking sequence ( $bCcA$ ) $a/C$  for half of the unit cell is faulted where the slant indicates a stacking fault, while the other half still remains in the normal ( $bCcA$ ) $aB$  stacking sequence. (For a more detailed description, a side view of this model can be found in Ref. 14.) The numbered atoms in this figure

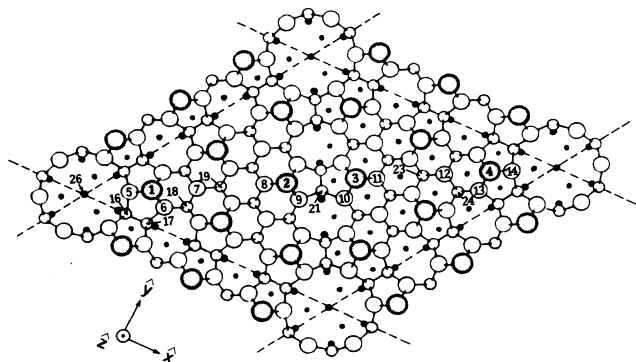


FIG. 1. Top view of the DAS model for the Si(111)-7×7 surface is shown. Atoms on (111) layers at increasing distances from the surface are indicated by circles of decreasing size. Large dotted circles represent adatoms situated at top sites. Larger open circles represent atoms in the stacking fault layer. Smaller open circles represent atoms in the dimer layer. Solid circles and dots represent atoms in the unreconstructed layers below the reconstructed surface. The 7×7 unit-cell boundaries are marked by dashed lines. The Cartesian coordinate system used for specifying the atomic coordinates in Table I is also shown.

are referred to in Table I, where the coordinates of relaxed atoms are given.

The merit of the DAS model is not *a priori* clear because of the delicate balance between the energy reduction arising from a low dangling-bond density and the energy increase resulting from large angular strains. The number of surface dangling bonds is reduced in two ways: (1) the number of surface-layer atoms is 42 as compared to 49 on the ideal surface, and (2) most surface dangling bonds (36) are eliminated by adatoms. It has now become clear that it is more favorable for adatoms to rest on top sites rather than on hollow sites when the system is completely relaxed.<sup>16</sup> The detailed balance between energy gain and loss requires a total-energy minimization calculation,<sup>15</sup> which is described in the following sections.

### III. METHOD OF CALCULATION

The semiempirical tight-binding based energy-minimization calculation has been described previously.<sup>17,18</sup> The method was originally designed to optimize atomic configurations for situations in which the total number of bonds in the system remained constant.<sup>17</sup> The method was later extended to deal with cases involving changes in the number of bonds.<sup>18</sup> The framework of  $sp^3$ -type semiempirical tight-binding formalism is very appealing because it can describe successfully many reconstructed surfaces for a wide range of materials with a small number of parameters which are predetermined from well-established quantities with very modest computational effort. Furthermore, it is very efficient for treating large systems with hundreds of atoms per cell. Therefore, we intend to retain this framework. The present work shows that it is possible to extend the semiempirical

TABLE I. Relaxed atomic positions for the adatom layer and the first three surface layers of the DAS model are given. All reduced coordinates ( $X, Y, Z$ ) are with respect to the Cartesian system indicated in Fig. 1, where the  $x$  axis is along the cubic  $[\bar{1}10]$  direction, the  $y$  axis is along the  $[\bar{1}\bar{1}2]$  direction, and the  $z$  axis is along the  $[111]$  outward normal to the surface. The actual atomic coordinates ( $x, y, z$ ) are related to ( $X, Y, Z$ ) by the scaling relations  $x = aX$ ,  $y = aY/\sqrt{3}$ ,  $z = aZ/\sqrt{24}$ , where  $a \approx 3.85$  Å is the  $1 \times 1$  surface hexagonal lattice constant, and  $a/\sqrt{24}$  is the bulk interplanar distance of  $\approx 0.78$  Å. The positions for equivalent atoms can be found via threefold symmetry operations about the lines ( $X, Y, Z$ ) specified by  $(0, 0, \xi)$ ,  $(3.5, 3.5, \xi)$ , and  $(7.0, 7.0, \xi)$  and from mirror symmetry about the plane passing through the long diagonal of the unit cell. The numbers given in column one (e.g., adatom 1, 2, etc.), correspond to the numbered atoms shown in Fig. 1. Atoms 15, 20, 22, and 25 are hidden from view by atoms 1, 2, 3, and 4, respectively. All third-layer atoms, except the one associated with the dangling bond at the corner of the unit cell, are below the appropriate second-layer atoms, and have not been numbered in Fig. 1.

		$X$	$Y$	$Z$
Adatoms	1	1.497	1.497	1.634
	2	4.494	4.494	1.538
	3	6.002	6.002	1.528
	4	9.007	9.007	1.564
First-layer atoms	5	1.026	1.026	-0.067
	6	1.962	0.990	-0.041
	7	2.480	2.480	0.369
	8	4.019	4.019	-0.144
	9	4.980	4.047	-0.108
	10	5.983	5.051	-0.122
	11	6.479	6.479	-0.134
	12	8.020	8.020	0.380
	13	9.028	8.052	-0.080
	14	9.478	9.478	-0.121
Second-layer atoms	15	1.504	1.504	-1.536
	16	1.163	0.005	-1.094
	17	1.794	0.007	-1.102
	18	2.493	1.499	-0.945
	19	2.969	2.969	-0.940
	20	4.496	4.496	-1.600
	21	5.404	4.779	-1.090
	22	6.004	6.004	-1.606
	23	7.530	7.530	-0.928
	24	8.505	7.509	-0.925
	25	8.998	8.998	-1.569
Third-layer atoms	26	0.000	0.000	-3.978
	27	1.501	1.501	-4.559
	28	1.005	-0.002	-4.044
	29	1.991	-0.001	-4.018
	30	2.500	1.500	-4.020
	31	2.997	2.997	-4.015
	32	4.499	4.499	-4.578
	33	5.497	4.511	-4.022
	34	6.000	6.000	-4.575
	35	7.500	7.500	-4.001
	36	8.503	7.498	-4.003
	37	9.000	9.000	-4.544

tight-binding method to describe surface systems with adatoms successfully. In the following paragraph, we quote the basic parameters used in previous calculations.

The nearest-neighbor four states per atom tight-binding model used in the calculations on Si is specified by the following parameters<sup>17</sup> (in eV):

$$\begin{aligned} V_{ss\sigma} &= -1.9375, & V_{pp\sigma} &= 3.050, \\ V_{sp\sigma} &= 1.745, & V_{pp\pi} &= -0.1075, \end{aligned} \quad (1)$$

and

$$\begin{aligned} E_s &= -5.25, \\ E_p &= 1.20. \end{aligned} \quad (2)$$

The choice of  $E_s$  and  $E_p$  sets the zero of energy at the bulk valence-band maximum. These parameters provide a reasonable description of the bulk occupied bands and an approximate description of the conduction bands. The variation of the total energy with atomic displacements and with changes in the number of bonds in the system is expressed as

$$\Delta D_{\text{tot}} = \sum_{n,\mathbf{k}} \Delta E_n(\mathbf{k}) + \sum_{\substack{i,j \\ i>j}} (U_1 \epsilon_{ij} + U_2 \epsilon_{ij}^2) + U_0 (\Delta N_{\text{bonds}}), \quad (3)$$

where the sum in the first term is over occupied one-electron states, and where the second term represents a semiempirical correction for the double counting of electron-electron interaction in the first term and includes the ion-ion interaction energy. The subscript  $i$  or  $j$  in Eq. (3) denotes a bond, and  $\epsilon_{ij}$  is the fractional change in bond length between atoms  $i$  and  $j$  from its reference value in bulk Si. The two empirical "spring" constants  $U_1$  and  $U_2$  were obtained by fitting the bulk elastic moduli and phonon frequencies<sup>17</sup> and are given by

$$\begin{aligned} U_1 &= -16.36 \text{ eV}, \\ U_2 &= 55.60 \text{ eV}. \end{aligned} \quad (4)$$

The last term of Eq. (3) is important only when comparing systems with different number of bonds  $N_{\text{bonds}}$ .  $U_0$  can be determined from the cohesive energy of the solid, i.e., from the change in total energy in going from the free atom to a bulk atom.<sup>18</sup> The value of  $U_0$  in Si is calculated to be (in eV)

$$U_0 = 4.1. \quad (5)$$

Equation (3) has been tested to be a good description for many systems of interest as long as the angular distortions and fractional bond changes from the appropriate bulk values are small. However, for some systems, in particular, for surfaces containing adatoms which involve large angular distortions, Eqs. (1)–(5) need to be modified. Several issues need to be considered. (1) The  $sp^3$ -type tight-binding matrix does not include  $d$  orbitals, so that discrepancies in the binding energy of adatoms can be seen when comparison with results obtained from other more accurate methods, e.g., density-functional calculations is made. (2) Within the  $sp^3$  framework, the atomic

levels  $E_s, E_p$  in Eq. (2) may not be a constant; they are likely to depend on coordination. (3) Since the previous systems of physical interest treated by the tight-binding method do not involve large angular distortions, it is legitimate to ask whether this formalism can treat systems with adatoms. Comparisons of tight-binding and *ab initio* local-density-functional results for "test" cases involving  $2 \times 2$  and  $\sqrt{3} \times \sqrt{3}$  adatom structures<sup>19</sup> indicate that the tight-binding method provides a good description of the surface and electronic structure but we have to go beyond Eqs. (1)–(5) in calculating the total energy.

The main problem with the original formalism Eq. (3) is that it assumes that the ion-ion repulsive energy parameter  $U_0$  is a constant between *any* pair of atoms. Although this assumption is legitimate for bulklike atoms, it is not necessarily true between surface atoms and adatoms. Because of the neglect of  $d$  states, the tight-binding method underestimates the binding energy of adatoms. The underestimation is larger for the top site than for the hollow site. This is to be expected since the angular distortions are much larger for the top-site geometry. In order to make tight-binding and density-functional results for the total energy consistent with each other, it is necessary to separate  $U_0$  into three categories: (1)  $U_0$  for bonds between atoms other than adatoms, with  $U_0 = 4.1$  eV as originally calculated in Eq. (5), (2)  $U_0^H$  for the bond between an adatom and an associated surface atom, and (3)  $U_0^T$  for the bond between an adatom and the second-layer atom directly under it. In order to compensate for the underestimation of adatom binding energies, the repulsive energies  $U_0^H$  and  $U_0^T$  should be smaller than  $U_0$ .  $U_0^H$  can be determined from the energy change in going from an ideal unrelaxed surface to a surface with an adatom placed at a hollow site.  $U_0^T$  can then be similarly determined from the energy change when the adatom is moved from the hollow site to a top site. The energy shift resulting from the placement of a Si adatom at a hollow site or at a top site has been calculated through self-consistent pseudopotential density-functional calculations.<sup>16,20</sup> Following the procedure outlined above, the values of  $U_0^H$  and  $U_0^T$  for Si(111) surface are calculated to be (in eV)

$$\begin{aligned} U_0^H &= 3.7, \\ U_0^T &= 2.6. \end{aligned} \quad (6)$$

The differences of  $U_0^H$  and  $U_0^T$  from  $U_0 = 4.1$  eV give an indication of how much the sum of the one electronic energies would have changed if  $d$  states had been included in the calculations.

Equation (3) can now be generalized to

$$\begin{aligned} \Delta E_{\text{tot}} &= \sum_{n,\mathbf{k}} \Delta E_n(\mathbf{k}) + \sum_{\substack{i,j \\ i>j}} (U_1 \epsilon_{ij} + U_2 \epsilon_{ij}^2) \\ &+ \Delta(U_0 N_0 + U_0^H N_H + U_0^T N_T), \end{aligned} \quad (7)$$

where  $N_0$  is the change of total number of bonds joining any atoms other than adatom.  $N_H$  is the change of total number of bonds joining any adatom and the associated surface layer atoms.  $N_T$  is the change of total number of

bonds joining an adatom and the second-layer atom right below that adatom. It is worth emphasizing that the extension from Eq. (3) to Eq. (7) only provides a better way of calculating the total energy; the surface electronic structure and the relaxation of the atomic structure are independent of  $U_0$ ,  $U_0^H$ , and  $U_0^T$  and come out exactly the same for the two approaches.

This method can be applied to other systems where  $d$  states are not crucial and do not dominate the electric structure. As long as we have reliable results available for "small" systems (e.g.,  $2 \times 2$  or  $\sqrt{3} \times \sqrt{3}$  surfaces), we can determine the new parameters in the semiempirical tight-binding formalism from these results. We can then carry out tight-binding calculations for much larger systems of up to a few hundreds of atoms.

#### IV. RESULTS OF CALCULATIONS

Calculations were carried out for two surfaces. The first one was for the ideal unrelaxed Si(111)-7×7 surface. We used a four-layer slab with hydrogen atoms at the bottom surface to saturate the Si dangling bonds. This system consists of 196 silicon atoms and 49 hydrogen atoms. If we consider  $s$  and  $p$  states for silicon atoms and only  $s$  states for hydrogen atoms, the tight-binding matrix to be diagonalized is  $833 \times 833$ . Since the superlattice unit cell is sufficiently large, one special point in the first Brillouin zone should be sufficient in the summation of the first term in Eq. (7). We have used the  $\Gamma$  point of the Brillouin zone for this purpose.

The second surface was the reconstructed DAS model of the Si(111)-7×7 surface as described in Sec. II. For a four-layer slab plus the adatom layer, we have 12 adatoms, 42 surface-layer atoms, 48 second-layer atoms, and 49 atoms for each of the remaining two layers.<sup>15</sup> Thus there are a total of 200 silicon atoms and 49 hydrogen atoms per unit cell. The corresponding secular matrix is  $849 \times 849$ . Hellmann-Feynman forces<sup>21,18</sup> were calculated in each step of the iteration process to determine the direction of motion of atoms which would result in a lowering of the total energy.

Table I gives the final geometry of the completely relaxed DAS model for the first three surface layers and for the adatom layer. It can be seen that all adatoms move substantially out towards the vacuum. The normal displacements are 0.41–0.50 Å away from the ideal tetrahedral positions. The bonds joining adatoms and surface-layer atoms are stretched by about 5.0–5.7% in comparison with the normal silicon-silicon bond length of 2.35 Å. The second-layer atoms beneath the adatoms are pushed down about 0.42–0.48 Å away from their ideal positions. The bond length between an adatom and the second-layer atom below it is stretched by about 4.4–5.7%. Third-layer atoms beneath the adatom are also seriously affected. This indicates that the present calculation can be improved if a larger unit cell is chosen so as to allow the deeper layers to relax also. The bond length between each pair of dimers along the boundaries of the triangular subunit cell is also stretched by 2–3%.

The surface energy of the completely relaxed Si(111)-7×7 DAS model is 0.403 eV per surface area lower than that of an ideal, unrelaxed Si(111) surface. A similar cal-

ulation was carried out for a Si(111)-5×5 DAS model; the corresponding energy shift is 0.395 eV per surface area.

Figure 2 shows the local density of states (at  $\Gamma$ ) for the adatoms, the first two layers of surface atoms and the exposed third-layer atom at the corner of the unit cell (total 103 atoms). The zero of energy is at the bulk valence-band maximum. The Fermi energy is calculated to be at  $\approx 0.3$  eV, as compared with the experimental value of 0.6 eV.<sup>22</sup> A larger sampling of the Brillouin zone is needed to calculate  $E_F$  more accurately. We can see from Fig. 2 that this surface is metallic, as predicted by experiment.<sup>8</sup> Figure 3 shows the local density of states of the above 103 surface atoms projected into atomic  $p_z$ ,  $s$ , and  $p_x + p_y$  states. Three prominent peaks can be seen from the projected  $p_z$  and  $p_x + p_y$  states:  $E_F$ ,  $E_F - 1.5$  eV,  $E_F - 3.1$  eV. In these plots the individual states at  $\Gamma$  have been broadened by the Gaussian function  $\exp(-E^2/2\sigma^2)$ , where  $\sigma = 0.3$  eV.

Recently a novel technique, current-imaging-tunneling spectroscopy (CITS), was reported.<sup>23</sup> This method uses real-space images of the tunneling current to measure directly the spatial distribution of surface states. Therefore it is now possible to identify the correspondence between surface electronic states and local geometrical configurations. CITS data were obtained for several important local geometrical configurations, such as adatoms, surface free atoms, adatom backbonding, corner atom associated with a dangling bond; the measured energies associated with these geometrical configurations are listed in Table II, for comparison with the calculated energies from the present work. The agreement between the two is very good. The different plots in Fig. 4 show the local

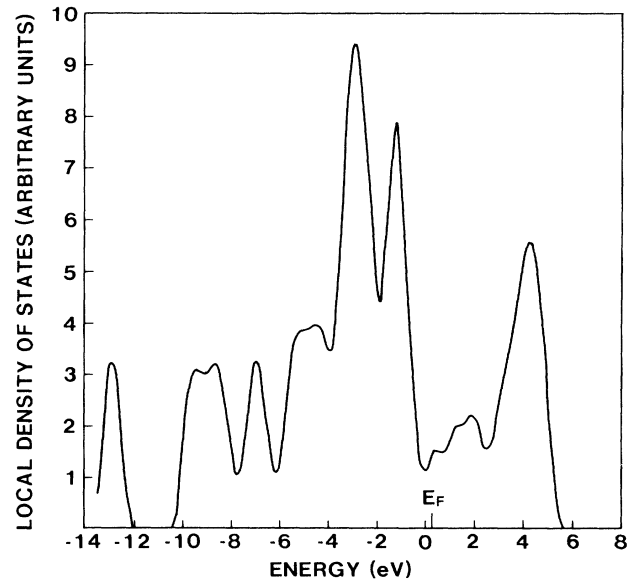


FIG. 2. Local density of states of 103 surface atoms (12 adatoms + 42 surface layer atoms + 48 second-layer atoms + one-third-layer atom with a dangling bond) is shown. The zero of energy is at the bulk valence-band maximum. The calculated Fermi energy is at  $\approx 0.3$  eV.

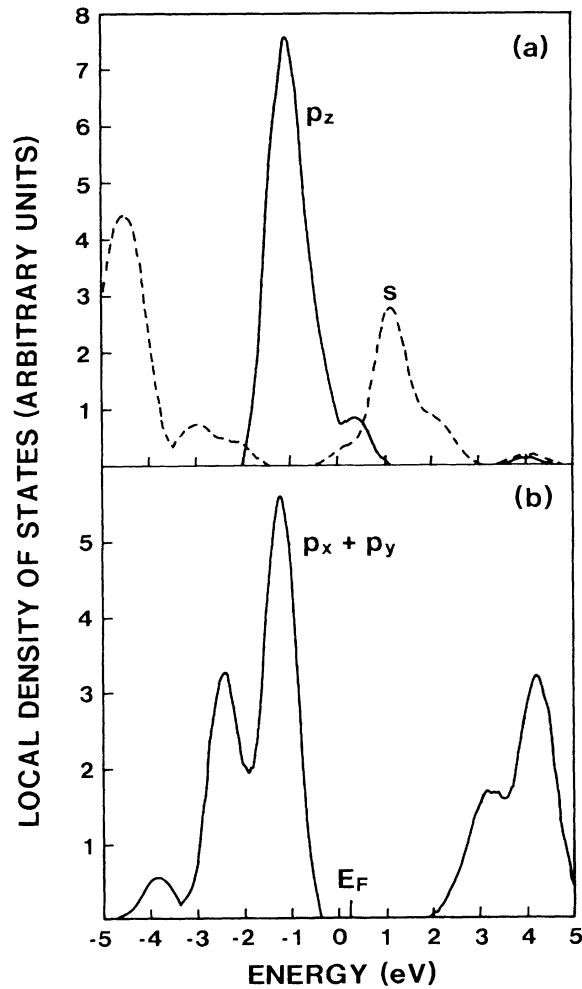


FIG. 3. Local density of states of the 103 surface atoms described in Fig. 2 caption projected into atomic  $p_z$  and  $s$  states is shown in (a); the projection into atomic  $p_x + p_y$  states is shown in (b).

TABLE II. Experimentally measured binding energies associated with four different local geometrical configurations are shown for comparison with the calculated energies for the same configurations from the present work.

	Experimental data <sup>a</sup>	Present calculation
Adatoms	$E_F - 0.2$ eV	$E_F$
	$E_F + 0.5$ eV	$E_F + 0.8$ eV
Six surface-free atoms	$E_F - 0.8$ eV	$E_F - 0.9$ eV
Adatom backbonding	$E_F - 1.7$ eV	$E_F - 1.5$ eV
Corner atom associated with a dangling bond	Between $E_F - 1.0$ and $E_F - 0.6$ eV	$E_F - 0.7$ eV

<sup>a</sup>Reference 23.

density of states originating from the following groups of atoms: the 12 adatoms, the 12 adatoms and their backbonds, the 6 free-surface atoms, the 18 dimer atoms, and the special corner atom. Table II and Fig. 4 identify the origin of the three surface states<sup>24,25</sup> for the Si(111)- $7 \times 7$  surface: the state at  $E_F - 0.2$  eV is due to adatoms, the one at  $E_F - 0.8$  eV arises from the free surface atoms, and the state at  $E_F - 1.8$  eV is localized on the backbonds of

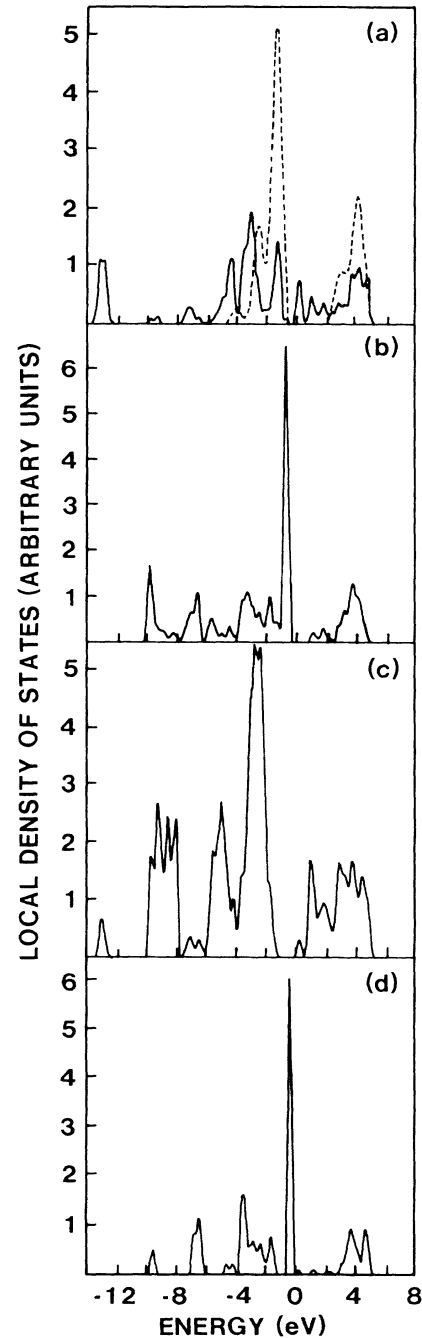


FIG. 4. Local density of states of (a) 12 adatoms (solid line); dashed line corresponds to 12 adatoms plus all the backbonds (60 atoms in total); (b) 6 surface-free atoms (i.e., the surface-layer atoms associated with dangling bonds); (c) 9 dimers; (d) the corner atom associated with the dangling bond.

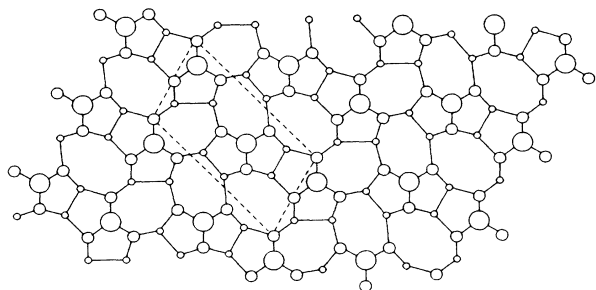


FIG. 5. Top view of the Si(111)- $c2\times8$  dimer-chain model. Atoms on (111) layers at increasing distances from the surface are indicated by circles of decreasing size. Largest open circles represent adatoms located on top sites. The  $c2\times8$  unit cell boundaries are shown by dashed lines.

the adatoms. These plots also indicate other states with energies further away from the Fermi energy.

#### V. CALCULATIONS OF Si(111)- $c2\times8$ DIMER-CHAIN MODEL

A similar calculation was also carried out for the dimer-chain model of the Si(111)- $c2\times8$  reconstructed surface proposed recently by Takayanagi and Tanishiro.<sup>26</sup> The atomic structure of this surface is shown in Fig. 5, where the large open circles represent adatoms, medium-size open circles represent surface atoms, and small open circles represent second-layer atoms. In each  $c2\times8$  unit cell, there are 4 adatoms and 12 surface-layer atoms. All adatoms are on top sites as in  $5\times5$  or  $7\times7$  DAS model but the local environment is not the same. Thus the total number of dangling bonds is reduced from 16 to 4. However, the energy reduction resulting from the lowering of the dangling-bond density is balanced by an increase in

the lattice strain energy. A tight-binding energy-minimization calculation indicates that the energy reduction of the completely relaxed  $c2\times8$  dimer-chain model of Si(111) surface from an ideal, unrelaxed Si(111)- $2\times8$  surface is only 0.18 eV per  $1\times1$  surface area. The relatively high surface energy of the new dimer-chain model for the  $c2\times8$  surface (0.22 eV per  $1\times1$  cell higher than for the  $7\times7$  DAS structure) suggests that other structures need to be investigated for this surface.

#### VI. SUMMARY

In summary, we have presented the results of the first energy-minimization calculations on the  $7\times7$ ,  $5\times5$  DAS models and  $c2\times8$  dimer-chain model of Si(111) surface. The surface energies per  $1\times1$  unit cell are calculated to be  $-0.403$ ,  $-0.395$ , and  $-0.18$ , respectively, relative to the Si(111) ideal, unrelaxed surface. The surface energy of the DAS model is 0.04 eV (per  $1\times1$  cell) lower than the  $\pi$ -bonded chain structure for the cleaved surface. Relaxation of a larger number of subsurface layers should make the  $7\times7$  surface even more favorable energetically. The Si(111)- $7\times7$  DAS model has the lowest surface energy ever calculated for a (111) surface. The completely relaxed atomic configurations and the local densities of surface states for this surface (which show excellent agreement with experimental measurements on the energy and atomic origin of the states) were also given.

#### ACKNOWLEDGMENTS

The authors wish to thank Dr. J. Northrup for giving us the local-density-functional results for the binding energy of adatoms on top and hollow sites prior to publication. This work was supported in part by the U.S. Office of Naval Research through Contract No. N00014-82-C-0244.

- <sup>1</sup>R. E. Schlier and H. E. Farnsworth, *J. Chem. Phys.* **30**, 917 (1959).
- <sup>2</sup>J. J. Lander and J. Morrison, *J. Appl. Phys.* **34**, 1403 (1963).
- <sup>3</sup>W. A. Harrison, *Surf. Sci.* **55**, 1 (1976).
- <sup>4</sup>G. Binning, H. Rohrer, Ch. Gerber, and E. Weibel, *Phys. Rev. Lett.* **50**, 120 (1983).
- <sup>5</sup>J. D. Levine, S. H. McFarlane, and P. Mark, *Phys. Rev. B* **16**, 5415 (1977).
- <sup>6</sup>D. J. Miller and D. Haneman, *J. Vac. Sci. Technol.* **16**, 1270 (1979).
- <sup>7</sup>L. C. Snyder, Z. Wasserman, and J. W. Moskowitz, *J. Vac. Sci. Technol.* **16**, 1266 (1979); L. C. Snyder, *Surf. Sci.* **140**, 101 (1984).
- <sup>8</sup>D. J. Chadi, R. S. Bauer, R. H. Williams, G. V. Hansson, R. Z. Bachrach, J. C. Mikkelsen Jr., F. Houzay, G. M. Guichar, R. Pinchaux, and Y. Pétroff, *Phys. Rev. Lett.* **44**, 799 (1980).
- <sup>9</sup>M. Aono, R. Souda, C. Oshima, and Y. Ishizawa, *Phys. Rev. Lett.* **51**, 801 (1983).
- <sup>10</sup>M. Tsukada and C. Satoko, *Surf. Sci.* **161**, 289 (1985).
- <sup>11</sup>E. G. McRae and C. W. Caldwell, *Phys. Rev. Lett.* **46**, 1632 (1981); E. G. McRae, *Phys. Rev. B* **28**, 2305 (1983).
- <sup>12</sup>P. A. Bennett, L. C. Feldman, Y. Kuk, E. G. McRae, and J. E. Rowe, *Phys. Rev. B* **28**, 3656 (1983).
- <sup>13</sup>K. Takayanagi, Y. Tanishiro, M. Takahashi, and S.

- Takahashi, *J. Vac. Sci. Technol. A* **3**, 1502 (1985).
- <sup>14</sup>K. Takayanagi, Y. Tanishiro, S. Takahashi, and M. Takahashi, *Surf. Sci.* **164**, 367 (1985).
- <sup>15</sup>Guo-Xin Qian and D. J. Chadi, *J. Vac. Sci. Technol. B* **4**, 1079 (1986).
- <sup>16</sup>J. E. Northrup, *Phys. Rev. Lett.* **57**, 154 (1986).
- <sup>17</sup>D. J. Chadi, *J. Vac. Sci. Technol.* **16**, 1290 (1979).
- <sup>18</sup>D. J. Chadi, *Phys. Rev. B* **29**, 785 (1984).
- <sup>19</sup>D. J. Chadi, *Phys. Rev. B* **30**, 4470 (1984).
- <sup>20</sup>J. E. Northrup and M. L. Cohen, *Phys. Rev. B* **29**, 1966 (1984).
- <sup>21</sup>H. Hellmann, *Einführung in die Quantentheorie* (Deuticke, Leipzig, 1937) p. 285; R. P. Feynman, *Phys. Rev.* **56**, 340 (1939).
- <sup>22</sup>F. J. Himpsel, G. Hollinger, and R. A. Pollak, *Phys. Rev. B* **28**, 7014 (1983).
- <sup>23</sup>R. J. Hamers, R. M. Tromp, and J. E. Demuth, *Phys. Rev. Lett.* **56**, 1972 (1986).
- <sup>24</sup>R. I. G. Uhrberg, G. V. Hansson, J. M. Nicholls, P. E. S. Persson, and S. A. Flodström, *Phys. Rev. B* **31**, 3805 (1985).
- <sup>25</sup>A. L. Wachs, T. Miller, T. C. Hsieh, A. P. Shapiro, and T.-C. Chiang, *Phys. Rev. B* **32**, 2326 (1985).
- <sup>26</sup>K. Takayanagi and Y. Tanishiro (unpublished).